

# Numerical Investigation on Wave Drag Reduction by Laser Energy Deposition

Xiaojing Yu\*, Hong Yan\* and Yong Wang\*\*  
Corresponding author: xj\_yu@nwpu.edu.cn

\* Northwestern Polytechnical University, China

\*\* Shanghai Space Propulsion Technology Research Institute, China

**Abstract:** A computational study was performed to analyze the flow field of multi-pulsed laser energy deposition before a Ma 8 bow shock. The interaction process of multiple blast waves and bow shock was analyzed. The influence of energy deposition frequency was compared. The results showed that, when the pulse frequency was lower than 25 kHz, the effects of each blast waves were almost isolated, and the pressure reduction was limited. When the pulse frequency reached 100 kHz, the superpose effects of blast waves were evident. A serial of wave transmission, reflection and amalgamation were appeared behind the bow shock, and greatly changed the shape of bow shock. The time-averaged pressure at the stagnation point was reduced to 72% of the baseline, which was benefit for the wave drag reduction.

*Keywords:* Wave Drag Reduction, Pulsed Energy Deposition, Numerical Simulation.

## 1 Introduction

Energy deposition, by injecting focused energy in front of a blunt body to alter the bow shock structure, was shown to be an effective way of wave drag reduction in supersonic flow [1~5]. Several studies on this method were carried out in recent years. Levin et al. [6] numerically studied the effects of energy deposition on aerodynamic drag and heat transfer of blunt body and predicted the limitation of drag reduction. Zheltovodov et al. [7] carried out a 2D unsteady numerical simulation for a Mach 3.45 flow. The results were compared with Adelgren et al. [8, 9] and Tretyakov et al. [10, 11] experiments. Riggins et al. [12, 13] numerically compared different wave drag reduction techniques. The results showed that the method of energy deposition had the greatest drag reduction capability and highest efficiency. Adelgren et al. [14] carried out a series of experiments to study the influence of energy deposition on hemisphere in Mach 3.45 flow. The stagnation pressure showed a 40% reduction. Erdem et al. [15, 16] carried out experiments in Mach 5 flow with arc discharge and analyzed the effect of different configuration. Sakai et al. [17], Sasoh et al. [18, 19] and Kim et al. [20, 21] carried out a series of numerical and experimental studied of energy deposition in Mach 2 flow and a 21% drag reduction was achieved in the experiments. Tate et al. [22] developed a non-equilibrium thermal chemical code to simulate the air ionization, and the interaction of blast wave and bow shock. Kremeyer [23] and Kremeyer et al. [24] studied the effects of pulsed energy lines on drag reduction. It showed advantages over pointed energy deposition.

The feasibility and the total effects of energy deposition were detailedly investigated in the previous studies. However, the interaction process and mechanism of blast wave and bow shock were not fully understood by now, especially in the multi-pulsed energy deposition condition. The objective of the present study was to further explore the flow field characteristics of wave drag reduction by multi-pulsed energy deposition before a cylinder in Mach 8 flow.

## 2 Flow Model and Numerical Method

A two dimensional flow was modeled based on the experiments [25, 26], in which a Mach 8 flow was past a cylinder with diameter of 76mm. The flow domain is sketched as Fig.1, where the origin of the coordinates lies on the stagnation point of the cylinder. The static pressure and temperature at freestream were 855Pa and 123.5 K, respectively.

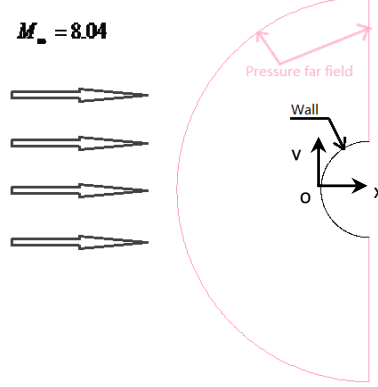


Figure 1: Flow configuration.

In the case of energy deposition, the laser energy was modeled as a sphere with uniformly distributed temperature and pressure, and was positioned in front of the cylinder on the x axis. The process of ionization was not considered in the present study.

The energy input by laser spot can be expressed by the following equation:

$$E = \rho_{\infty} c_v \Delta T V$$

where  $\rho_{\infty}$  is the freestream density,  $c_v$  is the specific heat at constant volume,  $\Delta T$  is the temperature increase due to energy deposition, and  $V$  is the laser focal volume, which was assumed as a sphere [27]. A dimensionless parameter was defined to evaluate the relative input energy to the flow:

$$\varepsilon = \frac{E}{E_l}$$

where  $E_l$  is the enthalpy of the local flow field without energy deposition, and can be expressed as:

$$E_l = \rho_{\infty} c_p T_{\infty} V$$

Two dimensional simulations were carried out with the commercial flow solver FLUENT. The second order accurate AUSM scheme was adopted for convective flux term and the first order implicit method was used for temporal discretization. The gradient reconstruction was based on node Green-Gauss method. Equations were solved using incomplete lower upper factorization (ILU), in conjunction with algebraic multigrid (AMG) method. The pressure far field condition was used for the inflow and outflow, where the Mach number, static pressure and temperature were fixed.

## 3 Results and Discussion

### 3.1 Baseline Flow

The flow without energy deposition was simulated first. The grids were uniformly distributed at one cylinder radius away from the surface, and then stretched along the radial direction with a ratio of 1.02. The grid number was 0.36 million.

Fig.2 showed the computed surface pressure compared with experiments [26]. The computational results were in good agreement with the experimental data. The theoretical standoff distance  $\Delta_{th}$  according to Ambrosio and Wortman [28] for 2D bow shock was:

$$\Delta_{th} = 0.386R \cdot \exp\left(\frac{4.67}{M_{\infty}^2}\right)$$

where  $R$  was the radius of the cylinder. For the case with  $M_\infty = 8$ ,  $R = 38\text{mm}$ ,  $\Delta_{th} = 15.8\text{mm}$ , the computed standoff distance was  $15.7\text{mm}$ , and its error was about  $0.6\%$  compared with the theoretical value. Fig.3 showed the contours of pressure and temperature, respectively. The pressure and temperature were increased greatly after the bow shock, which intensified the aerodynamic force and heating in the head region.

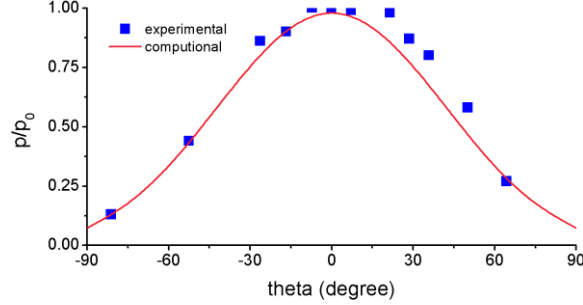


Figure 2: Surface pressure compared with experimental data.

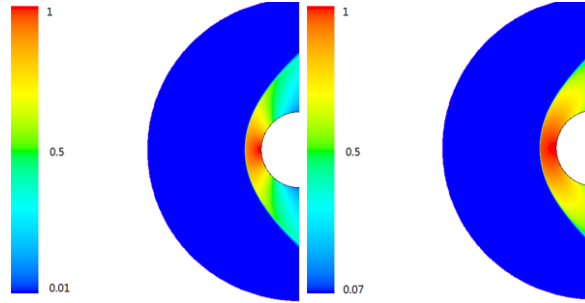


Figure 3: Normalized pressure (left) and temperature (right) contours of baseline flow.

## 3.2 Energy Deposition Flow

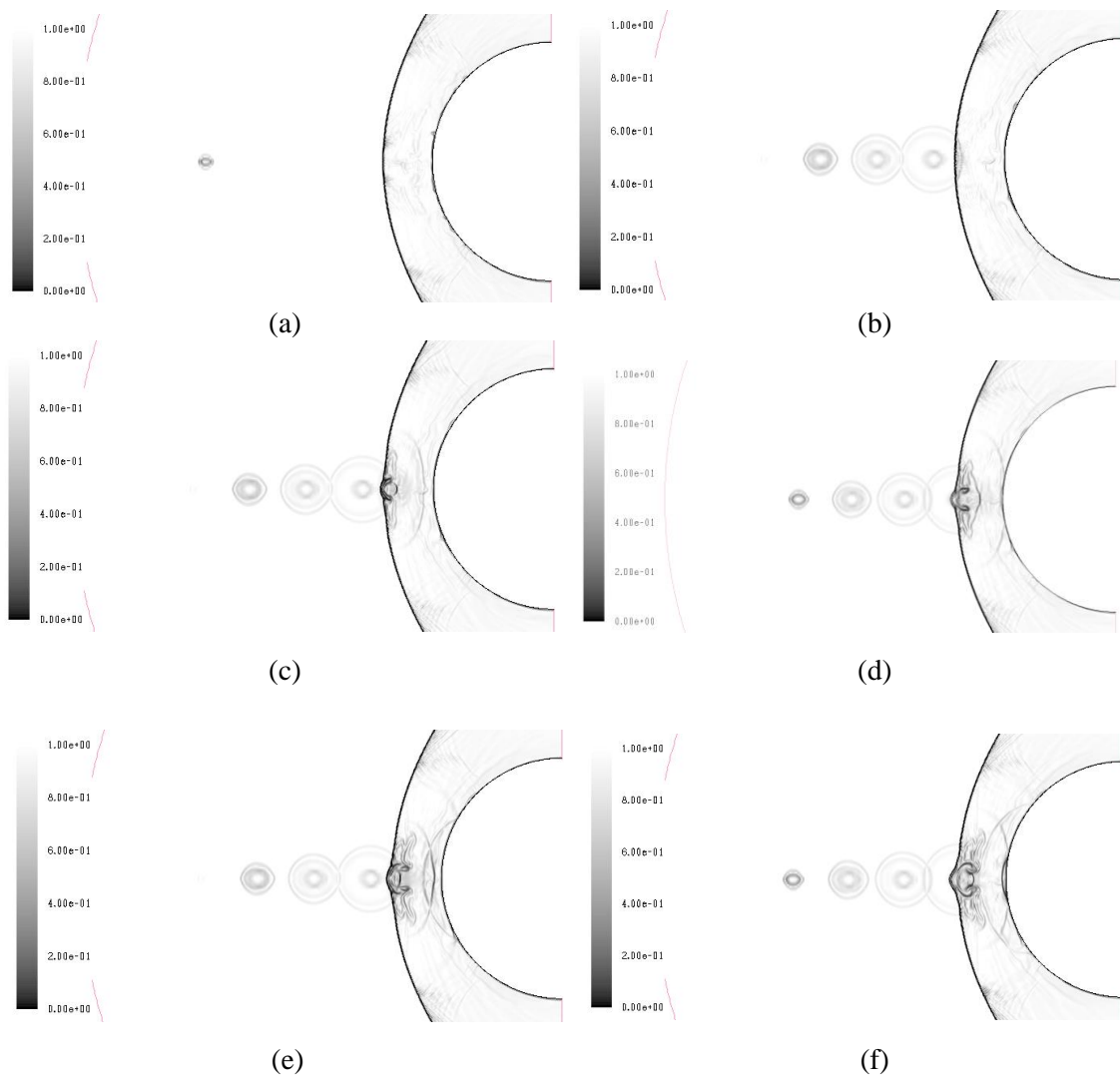
Once the baseline was obtained, an energy spot was deposited upstream of the bow shock. The energy level was  $\varepsilon = 10$  with the center of the focal zone located on the  $x$  axis and  $2R$  away from the cylinder. Three pulsing frequencies ( $f = 100, 25$  and  $10$  kHz) were studied. The time step was taken as  $0.5 e^{-8}$  s.

### 3.2.1 $f = 100\text{kHz}$

The numerical schlieren images were shown in Fig.4 to demonstrate the flow field structure during the interaction process.

At the initial stage (a), the first blast wave was formed due to the thermal spot caused by energy deposition pulse. It expanded and moved downstream towards the bow shock. At  $t \approx 30\mu\text{s}$  (b), the leading edge of the first blast wave encountered the bow shock, while the forth blast wave was just generated. As the blast wave moving forward, the blast wave and the bow shock mutual transit with each other. Because the temperature inside the blast wave was higher than the surrounding, and the Mach number was lower accordingly. The transmitted bow shock moved upstream and developed a convex shape, which was known as “lens-effect”. The leading edge of the blast wave transmitted into the shock layer. The density behind the bow shock was higher than the heated bubble. With the proceeding of the blast wave into the bow shock, it was compressed. When the transmitted bow shock met the trailing edge of the blast wave, additional waves emerged, which was reflected back towards the cylinder. At  $t \approx 40\mu\text{s}$  (c), the first blast wave was fully entered the shock layer and formed a concaved shell layer. At this moment, the leading edge of the second blast wave began to interact with the bow shock. At  $t \approx 44\mu\text{s}$  (d), the transmitted leading edge of the first blast wave impinged the wall of the cylinder. The second blast wave was gradually compressed in the shock layer, and its leading

edge was merged with the first reflected shock wave. At  $t \approx 50\mu s$  (e), the second blast wave was fully submerged into the shock layer, and was compressed. At  $t \approx 54\mu s$  (f), the leading edge of the second blast wave, combined with the first reflected shock wave, stroked the wall and reflected. The two compressed blast waves were amalgamated and a pair of vortex rings was formed. At the same time, the bow shock continued moving outward. At  $t \approx 60\mu s$  (g), the third blast wave was compressed and united with the anterior two to form a “mushroom-shaped” region. At  $t \approx 66\mu s$  (h), the third leading edge stroked the wall. And all the reflected waves from the wall united and formed a secondary bow shock liked wave before the wall. At  $t \approx 78\mu s$  (i), the fourth leading edge stroked the wall. After serials of wave transmission, reflection and amalgamation, the bow shock was transformed into a cone-shaped shock (j), and the standoff distance of stagnation point was increased to 18.3mm.



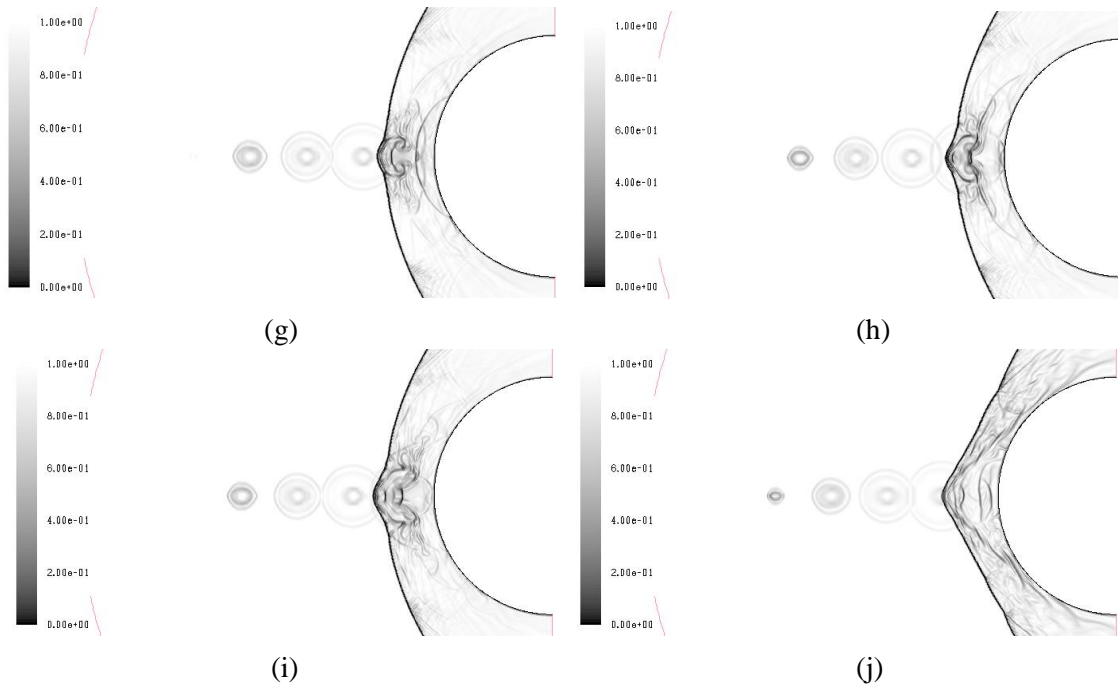


Figure 4: Numerical schlieren image of the flow process at  $f=100$  kHz.

The time-history of the normalized pressure at the stagnation point was shown in Fig.5. The first peak corresponded to the stage in Fig.4 (d) when the first leading edge of blast wave stoked the wall. After that, the following expansion wave caused the pressure to decrease. The second peak corresponded to the stage in Fig.4 (f), which was the combined effects of second blast wave leading edge and reflect shock wave. The following pressure drop was also the effects of expansion wave. The third and fourth peaks corresponded to Fig.4 (h) and (i) respectively. The pressure was vibrated because of the continually striking of compression and expansion waves. The time-averaged pressure at the stagnation point was 72% of the baseline, which was benefit for the wave drag reduction.

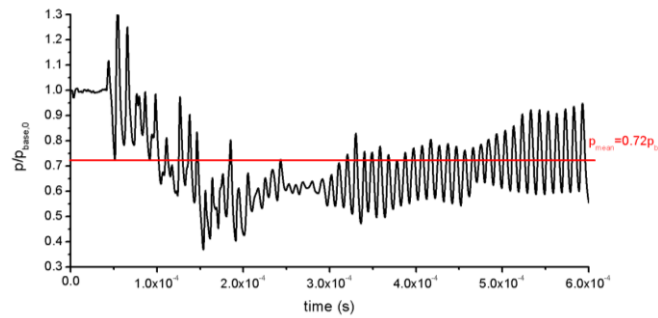
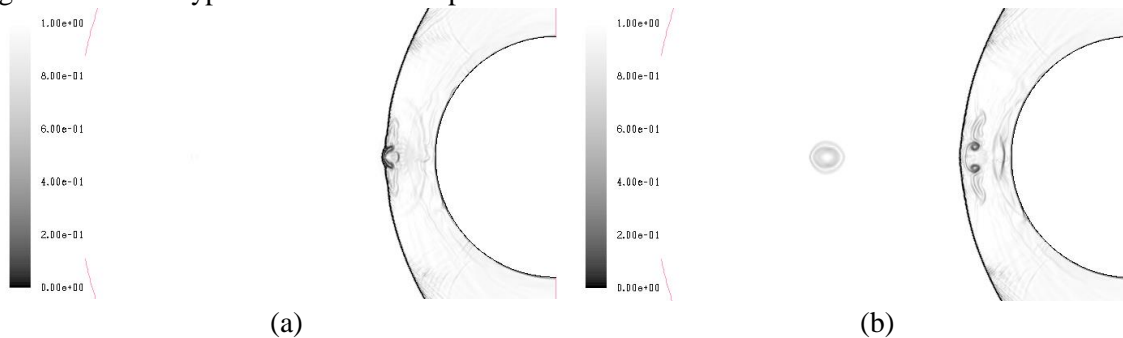


Figure 5: Time history of the pressure at stagnation point at  $f=100$  kHz.

### 3.2.2 $f=25$ kHz

When the frequency was reduced, the flow characteristics were quite different from the previous case. Fig.6 showed the typical moment of the process.



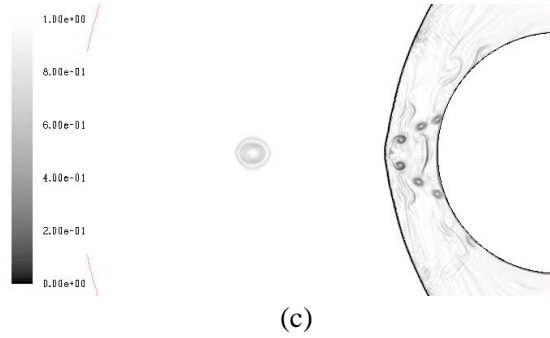


Figure 6: Numerical schlieren image of the flow process at  $f=25$  kHz.

Fig.6 (a) indicated that, the first blast wave was submerged and compressed by the bow shock like the previous case, while the next blast wave hasn't been generated yet. This was because the intervals between the pulsed were relatively long. When the second blast wave appeared (b), the first compressed waves rolled up to form a pair of counter-rotating vortex in the shock layer. With the flow proceeded and reached a quasi-steady state (c), three pairs of vortexes exist behind the bow shock. The flow field structure was not complicated as the  $f=100$  kHz case, and the superposed effect of multiple pulses were not evident. Fig.7 showed the time history of stagnation point pressure, it could be seen that the time-averaged pressure was 91% of the baseline, which was much lower than the previous case.

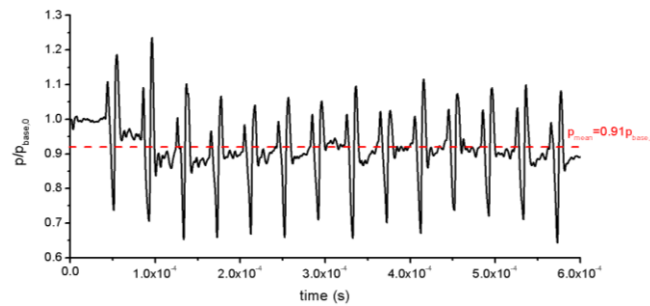


Figure 7: Time history of the pressure at stagnation point at  $f=25$  kHz.

### 3.2.3 $f=10$ kHz

When the pulse frequency was further reduced to 10 kHz, the effect of each pulse was almost isolated, as indicated in Fig.8. In the quasi-steady state, only a pair of vortex existed in the central part of the bow shock, and the previous pair of vortex was slide down along the cylinder wall. The time history of stagnation point pressure (Fig.9) showed that, the time-averaged pressure was 96% of the baseline, which was almost the same with single pulsed condition and was inefficient.

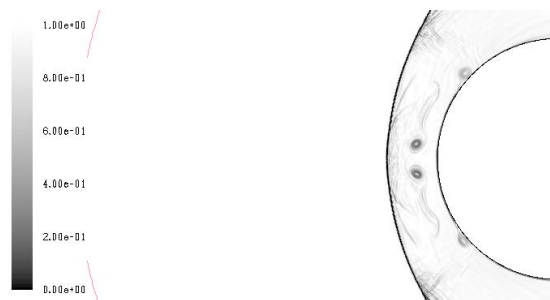


Figure 8: Numerical schlieren image of the flow process at  $f=10$  kHz.

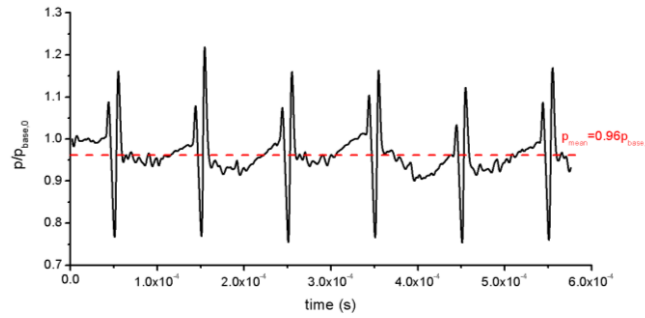


Figure 9: Time history of the pressure at stagnation point at  $f=10$  kHz.

### 3 Conclusion

The flow characteristics of multi-pulsed energy deposition before a Mach 8 bow shock were numerically analyzed. The results showed that, when the frequency was low, as in the case of 10 kHz, the effect of each pulse was isolated. The disturbance of one blast wave had trivial influence on other blast waves. The pressure reduction was as low as that in single pulse condition. In the case of 25 kHz, there existed three pairs of vortex behind the bow shock in quasi-steady state. The influences of blast waves were not superposed, and the reduction of pressure at stagnation point was limited. In the case of 100 kHz, the interaction of each pulses were evident and the flow field was complicate. The convex shape of bow shock, the superpose effect of compressed blast waves, and the expansion waves were the main structures that influenced the pressure fluctuation. In the present case, the stagnation point pressure was reduce to 72% of the baseline at frequency of 100 kHz and  $\varepsilon = 10$ , with the energy deposition position located  $2R$  away from the cylinder.

### Acknowledgements

This work is supported by the Natural Science Foundation of China (No.51506178) and Aeronautical Science Foundation of China (No. 2015ZA53009).

### References

- [1] P. K. Tretyakov, V.Fomin, and V. I. Yakovlev, New principle of control of aerophysical process, Proc. International Conference on the Methods of Aerophysical Research, 1996: 210-220.
- [2] G. G. Chernyi, The impact of electromagnetic energy addition to air near the flying body on its aerodynamics characteristics, Proceedings of the 2nd Weakly Ionized Gases Workshop,, 1998:1-31.
- [3] A. A. Zheltovodov, Development of the studies on energy deposition for application to the problems of supersonic aerodynamics, Preprint No. 10-2002, Institute of Theoretical and Applied Mechanics, Russian Academy of Sciences, Siberian Branch, Novosibirsk, 2002.
- [4] D. D. Knight, V. Kuchinskiy, A. Kuranov, and E. Sheikin, Survey of aerodynamic flow control at high speed by energy deposition, AIAA Paper, 2003-0525.
- [5] V. Fomin, P. Tretyakov, and J. P. Taran, Flow control using various plasma and aerodynamic approaches (shot review), Aerosp. Sci. and Techol., No.8,2004:411-421.
- [6] V. A. Levin, V. G. Gromov, and N. E. Afonina, Numerical analysis of the effect of local energy supply on the aerodynamic drag and heat transfer of a spherically blunted body in a supersonic air flow, J. App. Mech. Tech. Phy., Vol. 41, No. 5, 2000:915-922.
- [7] A. A. Zheltovodov, E. A. Pimonov, and D. D. Knight, Energy deposition influence on supersonic flow over axisymmetric bodies, AIAA Paper,, 2007-1230.
- [8] R. G. Adelgren, G. Elliott, D. D. Knight, A. A. Zheltovodov, and T. Beutner, Energy deposition

- in supersonic flow, AIAA Paper, 2001-0885.
- [9] R. G. Adelgren, H. Yan, G. Elliott, D. D. Knight, T. Beutner, A. A. Zheltovodov, and M. Ivanov, Localized flow control by laser energy deposition applied to Edney IV shock impingement and intersection shocks, AIAA Paper, 2003-0031.
- [10] P. K. Tretyakov, A. F. Garanin, G. P. Grachev, V. L. Kraynev, A. G. Ponomarenko, V. N. Tishenko, and V. L. Yakovlev, The supersonic flow control over the bodies with the use of power optical pulsating discharge, Dokladi Akademii Nauk (DNA), Vol. 351, No. 3, 1996: 339-340.
- [11] P. K. Tretyakov, A. F. Garanin, and V.I. Yakovlev, Investigation of local laser energy release influence on supersonic flow by methods of aerophysical experiments, Proc: International Conference on the Methods of Aerophysical Research, 1996: 200-204.
- [12] D. W. Riggins, H. F. Nelson, and E. Johnson, Blunt body wave drag reduction using focused energy deposition, AIAA Paper, 98-27875.
- [13] D. W. Riggins, J. T. Barnett, and T. T. Taylor, Drag Reduction and Heat Transfer Mitigation Techniques for Blunt Bodies in Hypersonic Flight, AIAA Paper, 2003-6968.
- [14] R. G. Adelgren, H. Yan, G. S. Elliott and D. D. Knight, Drag and total power reduction for artificial heat input in front of hypersonic blunt bodies, AIAA J., Vol. 43, No.2, 2005: 256-269.
- [15] E. Erdem, L. Yang, and K. Kontis, Drag Reduction by Energy Deposition in Hypersonic Flows, AIAA Paper, 2009-7374.
- [16] E. Erdem, L. Yang, and K. Kontis, Drag Reduction Studies by Steady Energy Deposition at Mach 5, AIAA Paper, 2011-1027.
- [17] T. Sakai, Y. Sekiya, M. Rosli, A. Matsuda, and A. Sasoh, Unsteady interaction of blunt bodies with laser induced plasma in a supersonic Flow, AIAA Paper, 2008-3794.
- [18] A. Sasoh, Y. Sekiya, T. Sakai, J. H. Kim and A. Matsuda, Drag reduction of blunt body in a supersonic flow with laser energy depositions, AIAA Paper, 2009-1533.
- [19] A. Sasoh, Y. Sekiya, T. Sakai, J. H. Kim, and A. Matsuda, Supersonic drag reduction with repetitive laser pulses through a blunt body, AIAA J., Vlo.48, No.12, 2010:2811-2817.
- [20] J. H. Kim, A. Matsuda, T. Sakai, and A. Sasoh, Drag reduction with high-frequency repetitive side-on laser pulse energy depositions, AIAA Paper, 2010-5104.
- [21] J. H. Kim, A. Matsuda, T. Sakai and A. Sasoh, Wave drag reduction with acting spike induced by laser-pulse energy depositions, AIAA J., Vol. 49, No.9, 2011:2076-2078.
- [22] M. Tate, Y. Ogino, and N. Ohnishi, Thermochemical nonequilibrium flow computation of drag reduction by pulsed laser, AIAA Paper, 2010-1535.
- [23] K. Kremeyer, Lines of pulsed energy for supersonic/hypersonic drag reduction, AIAA Paper, 2004-984.
- [24] K. Kremeyer, K. Sebastian, and C. W. Shu, Computational Study of Shock Mitigation and Drag Reduction by Pulsed Energy Lines, AIAA J., Vol.44, No.8, 2006:1720-1731.
- [25] M. S. Holden, and J. R. Moselle, A database of aerothermal measurements in hypersonic flow for CFD validation, AIAA Paper, 92-4023.
- [26] A.R. Wieting, and M. S. Holden, Experimental shock-wave interference heating on a cylinder at Mach 6 and 8, AIAA J., Vlo.27, No.11, 2089:1557-1565.
- [27] H. Yan, R. G. Adelgren, M. Boguszko, and D. D. Knight, Laser energy deposition in quiescent air, AIAA J., Vlo.41, No.10, 2003:1988-1995.
- [28] A. Ambrosio, and A. Wortman, Stagnation point shock detachment distance for flow around spheres and cylinders, ARS J., 32, 1962.